

Effect of the structural anisotropy and lateral strain on the surface phonons of monolayer xenon on Cu(110)

P. Zeppenfeld, M. Büchel, R. David, and G. Comsa

Institut für Grenzflächenforschung und Vakuumphysik, Forschungszentrum Jülich, D-52425 Jülich, Germany

C. Ramseyer and C. Girardet

Laboratoire de Physique Moléculaire, URA CNRS 772, Université de Franche-Comté, F-25030 Besançon Cedex, France

(Received 1 July 1994)

The phonon-dispersion curves for a xenon monolayer adsorbed on Cu(110) have been measured using inelastic He scattering. The size and geometry of the substrate unit cell introduces an anisotropic distortion of the xenon monolayer, which is reflected in a strong deformation of the phonon-dispersion curves with respect to the floating two-dimensional (2D) xenon layer. This effect is reproduced in a 2D phonon calculation, based on the Lennard-Jones Xe pair potential. In this way a microscopic relationship between lattice strain, force constants, and surface stress can be established.

Collective vibrations (phonons) at crystal surfaces critically depend on the relative arrangement of the constituting atoms or molecules. Therefore, the phonon energies and dispersion curves can, in principle, be used to extract additional information on the structure of surfaces and adsorbed layers. As an example, the evolution of the phonon dispersion of monolayer and multilayer rare-gas films on Ag(111) (Ref. 1) and Pt(111) (Ref. 2) has been used to confirm the layer-by-layer growth of these films. The phonons are particularly sensitive to changes that affect the overall symmetry of the surface since they are usually connected with the appearance of additional phonon branches. This has been observed, e.g., in the case of a surface reconstruction.³ However, more gradual changes such as the continuous distortion of the structure have, until now, been accounted for only by the empirical fitting of force constants or by *ab initio* calculations. Only in a few cases have explicit rules been proposed to describe the effect of a lattice distortion on the interatomic coupling.⁴

Here we present a combined experimental and theoretical investigation of the surface phonons of monolayer Xe on Cu(110) for which the relationship between lattice distortion and phonon dispersion can be understood purely on the basis of the interatomic potentials. The phonon dynamics of this quasi-two-dimensional (2D) system is rather simple and can be treated quantitatively because the lateral Xe-Xe interaction is well known from the gas phase and the dynamic coupling to the underlying substrate is easily accounted for. At the same time, the structure of the Xe monolayer is highly anisotropic and strongly deformed with respect to the hexagonally close-packed "floating" Xe layer.

The phonon-dispersion curves were obtained using inelastic He scattering, which allows the low-phonon frequencies of the Xe monolayer (a few meV) to be measured with a precision of about 0.2 meV. The experimental setup is described in detail in Ref. 5. The phonon-dispersion curves $\hbar\omega(Q)$ (i.e., the phonon energies as a function of the parallel wave-vector transfer Q) were obtained from He time-of-flight (TOF) spectra taken at

different scattering angles (ϑ_i, ϑ_f). The sample is a high-quality single-crystal Cu(110) surface with a surface miscut angle $< 0.2^\circ$. It was cleaned *in situ* by repeated cycles of sputtering with Ar ions and heating to about 1000 K. The quality of the surface was routinely checked by He diffraction, which constitutes a sensitive measure for surface defects and impurities.⁶ The base pressure in the scattering chamber is in the low 10^{-11} -mbar range.

The Xe monolayer was adsorbed by exposing the cold Cu(110) surface (≤ 50 K) to a Xe partial pressure or by means of a doser positioned in front of the sample. The Xe coverage can be easily controlled by monitoring the specularly reflected He intensity.⁷ When the monolayer coverage was reached, the Xe gas was pumped off; the surface was carefully annealed around 55 K and then cooled to 20 K where most of the inelastic He-scattering experiments were carried out. The structure of the Xe monolayer was characterized by He diffraction. In the temperature regime studied ($20 \text{ K} \leq T \leq 60 \text{ K}$), high-order commensurate ($n \times 2$) structures are formed, where n can reach various values between 12 and 30 depending on surface temperature. The details of the structure analysis will be presented elsewhere. We find that the most stable of these structures is the (26×2) structure shown in Fig. 1(a): The Xe atoms are arranged in a quasihexagonal lattice which, however, is strongly deformed as a consequence of the anisotropy of the underlying rectangular Cu(110) lattice. Along the $[001]$ direction, the Xe atomic rows are in perfect registry with the underlying substrate, while along the $[1\bar{1}0]$ direction, 15 Xe atoms cover 26 Cu lattice distances: $15a_{\text{Xe}} = 26a_{\text{Cu}}$. With the Cu nearest-neighbor distance being $a_{\text{Cu}} = 2.55 \text{ \AA}$, the distance between neighboring Xe atoms along the $[1\bar{1}0]$ direction becomes $a_{\text{Xe}} = 4.42 \text{ \AA}$. Across the Cu close-packed rows, the distance between neighboring Xe atoms is only $b_{\text{Xe}} = 4.23 \text{ \AA}$, as a consequence of the separation between Cu atomic rows of $b_{\text{Cu}} = 3.61 \text{ \AA}$ [Fig. 1(a)]. Therefore, the Xe lattice is strongly distorted with respect to the perfectly hexagonal lattice of a floating 2D Xe layer in which $a_{\text{Xe}} = b_{\text{Xe}} = 4.36 \text{ \AA}$ [Fig. 1(b)].

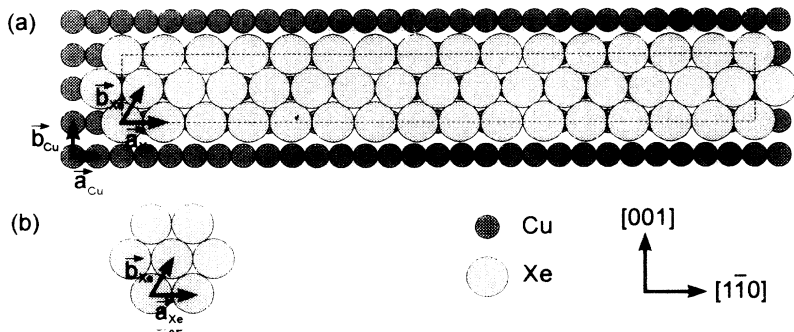


FIG. 1. (a) Model of the (26×2) HOC phase of a Xe monolayer on Cu(110). The xenon atoms are arranged in a quasi-hexagonal structure; the HOC unit cell is indicated by the dashed lines. In order to fit on the rectangular substrate lattice the Xe layer is compressed along the $[001]$ direction and stretched along the $[1\bar{1}0]$ direction with respect to the floating 2D Xe phase ($a_{Xe} = 4.36 \text{ \AA}$) shown in (b). It is not known whether the Xe atoms on Cu(110) are bound on top of the Cu rows, as shown here, or in the Cu troughs.

The He-scattering experiments reported below were performed on this most stable (26×2) high-order commensurate (HOC) phase. Figure 2 shows a typical energy spectrum of the He atoms scattered from the Xe monolayer along the $[1\bar{1}0]$ direction. Besides the elastically scattered beam ($\Delta E = 0$), phonon peaks at energies 2.5, 3.75, and 5.0 meV can be clearly distinguished. The dominant feature at 2.5 meV is attributed to the Xe vibration perpendicular to the surface. This value is in good agreement with the one observed by Mason and Williams ten years ago.⁸ The phonon loss at 5.0 meV corresponds to the double excitation of this almost dispersionless vibrational mode. The third feature has not been observed previously. As we will see below it can be attributed to the longitudinal Xe phonon. The dispersion curves of the different phonon modes along the $[1\bar{1}0]$ direction, obtained from a large number of TOF spectra are plotted in Fig. 3. Again three vibrational modes can be distinguished. (i) The first is the vertical Xe mode \perp (Einstein mode), which is almost dispersionless for $Q > 0.3 \text{ \AA}^{-1}$. For smaller wave vectors a hybridization with the surface Rayleigh wave (R) is observed leading to an avoided crossing of the corresponding branches H_1 and H_2 . This phenomenon is well known from other rare-gas overlayers^{9,10} and can be explained quantitatively by the dynamic coupling between substrate and adlayer.^{11,12} (ii) The second vibrational mode is the double excitation of the quasidispersionless mode, which leads to

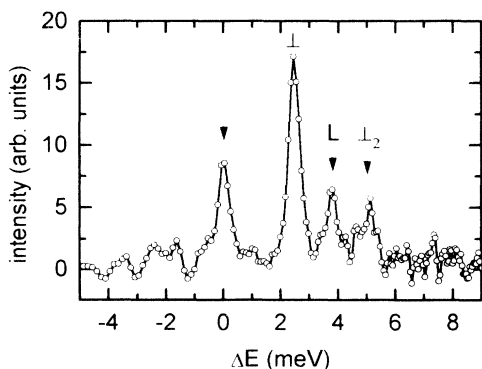


FIG. 2. He energy-loss spectrum of a Xe monolayer physisorbed on Cu(110) taken along the $[1\bar{1}0]$ direction (primary He energy 18.2 meV ; $\vartheta_i = 36.0^\circ$, $\vartheta_f = 54.0^\circ$). The energy losses at $\Delta E = 2.5$ and 5 meV , respectively, correspond to the single (\perp) and double (\perp_2) excitation of the Xe vibration perpendicular to the substrate surface. The energy loss at 3.75 meV ($Q = 0.80 \text{ \AA}^{-1}$) is attributed to the Xe longitudinal mode (L).

a narrow phonon band \perp_2 centered at around 5 meV . (iii) The third mode is the longitudinal Xe mode L in which the Xe atoms are displaced parallel to the $[1\bar{1}0]$ direction in the surface plane. To our knowledge, this is the first time that the dispersion of the longitudinal phonon mode of a physisorbed monolayer has been measured *directly*.¹³ It is this longitudinal mode that will be affected most sensitively by the lattice distortion (lateral strain) of the Xe monolayer.

In order to give a quantitative account of the Xe phonon dynamics, we have performed model calculations of the 2D Xe layer. The monolayer was coupled to a rigid, flat substrate. Hence, the effect of the substrate was described by a single force constant ϕ''_{Xe-Cu} acting on each Xe atom in the direction perpendicular to the surface. The value of ϕ''_{Xe-Cu} was chosen to give a phonon energy $\hbar\omega = \hbar\sqrt{\phi''_{Xe-Cu}/M_{Xe}} = 2.5 \text{ meV}$. The Xe-Xe interaction is modeled by pairwise Lennard-Jones potentials with potential parameters $\epsilon = 24.87 \text{ meV}$ and $\sigma = 3.885 \text{ \AA}$ adopted from the gas-phase potential.¹⁴ Using the rigid-substrate assumption, we cannot reproduce the hybridization between adlayer and substrate phonons in the re-

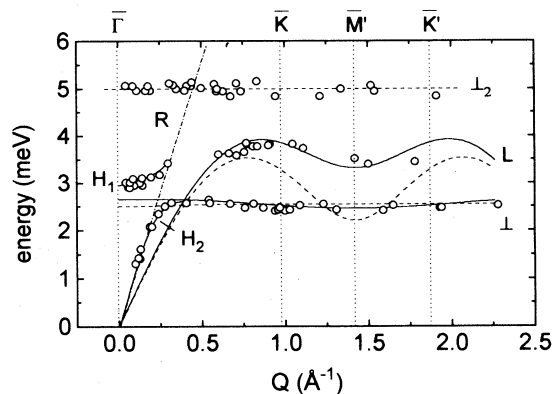


FIG. 3. Phonon-dispersion curves of the Xe monolayer along the $[1\bar{1}0]$ direction. Open circles are experimental data obtained from He energy-loss spectra (Fig. 2). The dashed lines are the calculated dispersion curves \perp and L assuming a perfectly hexagonal Xe lattice ($a_{Xe} = b_{Xe} = 4.36 \text{ \AA}$). The solid lines are the dispersion curves with the actual lattice distortion taken into account ($a_{Xe} = 4.42 \text{ \AA}$, $b_{Xe} = 4.23 \text{ \AA}$). The dash-dotted line (R) marks the substrate Rayleigh wave. The hybridization of the \perp mode and the Rayleigh wave leads to the avoided crossing of the phonon branches H_1 and H_2 . $\bar{\Gamma}$, \bar{K} , \bar{M}' , and \bar{K}' indicate the high-symmetry points of the reciprocal lattice of the distorted Xe structure.

gion where the Xe perpendicular mode intersects with the Cu(110) Rayleigh wave. For the present purpose, this is not important since the dispersion of the Xe perpendicular mode for $Q > 0.3 \text{ \AA}^{-1}$ and the longitudinal mode are not affected by the dynamical coupling, anyway. As far as the lateral interaction is concerned, the gas-phase Lennard-Jones potentials have proven in the past to be well suited for the description of the phonon dynamics of thin rare-gas films.⁹ Using these interactions, the dynamical matrix of the Xe monolayer was calculated by summing the pairwise contributions over the entire 2D Xe lattice. Then the 3×3 matrix was diagonalized and the dispersion curves for the three orthogonal phonon modes were obtained. Calculations were performed for two different configurations of the Xe layer; the ideal 2D floating phase and the distorted (strained) Xe layer, respectively.

The results for the two Xe structures are shown together with the experimental data in Fig. 3. The first calculation assumes a perfectly hexagonal 2D Xe phase in which the energy per Xe atom is minimized [$a_{\text{Xe}} = b_{\text{Xe}} = 4.36 \text{ \AA}$, see Fig. 1(b)]. The phonon-dispersion curves for this phase are given by the dashed lines in Fig. 3. Because the transverse mode is not accessible to our experiment and for reasons of clarity, only the vertically and longitudinally polarized modes are plotted. The perpendicular mode is almost dispersionless and fits the experimental data points by construction. For the longitudinal mode, however, the calculation for the perfect hexagonal structure cannot describe the experiment at all. The dispersion curve lies well below the experimental one and, most obviously, the modulation of the longitudinal mode (i.e., the difference of the phonon energies at $Q \approx 0.8 \text{ \AA}^{-1}$ and at the \bar{M}' point of the Brillouin zone) is much larger than observed (1.3 meV instead of 0.5 meV).

The situation changes completely if the Xe lattice is distorted to match the actual structure on Cu(110). Using $a_{\text{Xe}} = 4.42 \text{ \AA}$ and $b_{\text{Xe}} = 4.23 \text{ \AA}$, the phonon-dispersion curves for the strained Xe monolayer were calculated and are plotted as solid lines in Fig. 3. Now the agreement with the experimental results is excellent. In the distorted configuration the separation between neighboring Xe atoms deviates significantly from the binding distance of the Lennard-Jones pair potential. This leads to a change of the force constants and introduces lateral surface-stress terms into the dynamical matrix. The stress is tensile along the [001] direction (with the propensity of the Xe layer to expand along that direction) and compressive along the $[1\bar{1}0]$ direction. Similar to the tightening of a guitar string, the stress affects the phonon frequency of the modes polarized along a perpendicular direction. For instance, the tensile stress along the [001] direction will affect the perpendicular Xe vibration (introducing a finite dispersion in the \perp mode) as well as the longitudinal mode along the $[1\bar{1}0]$ direction. The effect of the lattice distortion is most pronounced for the longitudinal mode and explains the anomalous dispersion of this mode observed in the experiment (Fig. 3). In addition, the calculated curve for the perpendicular mode \perp now exhibits a slight dispersion of about 0.2 meV, which also is in good agreement with the experimental data.

However, it would not have been possible to quantify the effect of the lattice distortion on the basis of the dispersion of the \perp mode alone. The experimental errors as well as the effect of the avoided crossing with the Rayleigh wave are both of the same size as the strain-induced dispersion. This demonstrates the importance to measure the longitudinal phonons if a relationship between lateral structural changes and the phonon dynamics is to be investigated.

From the ability of the above calculation to reproduce the experimental data, we can conclude that the interatomic force constants and stress in the distorted Xe phase are, indeed, accurately described by the second and first derivatives of the Xe Lennard-Jones pair potential evaluated at the new (nonequilibrium) atomic positions within the distorted structure.

The effect of a continuous distortion along the [001] and $[1\bar{1}0]$ direction on the characteristic phonon frequencies of the perpendicular and longitudinal modes is given in Fig. 4. The most notable feature upon distortion of the perfectly hexagonal lattice towards the final structure is the effective reduction of the modulation of the longitudinal mode (given by the energy difference between the lower- and upper-triangle curves). For even larger distortions ($a_{\text{Xe}} > 4.6 \text{ \AA}$), the modulation even vanishes completely. This would be the case, e.g., for a $c(2 \times 2)$ Xe commensurate phase ($a_{\text{Xe}} = 5.1 \text{ \AA}$), which has been discussed previously.^{15,16} It is also apparent from Fig. 4 that the stress due to the compression of the structure along the [001] direction and the dilatation along the $[1\bar{1}0]$ direction act concurrently on the Xe perpendicular mode and, therefore, tend to cancel each other.

We would like to close with a discussion of the effect of the substrate corrugation on the phonon dynamics. In fact, the Xe adlayer is strained and the distorted lattice is

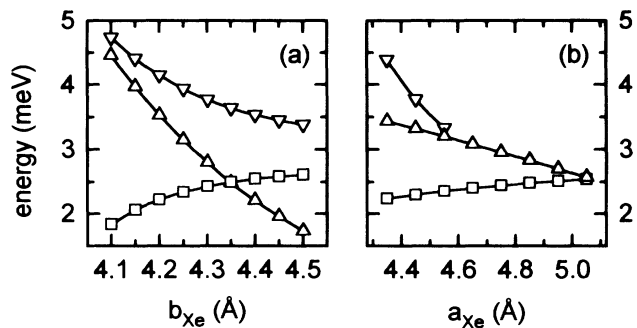


FIG. 4. Calculated variation of the characteristic phonon frequencies as a function of the distortion of the Xe layer. Different symbols correspond to the phonon energy of the perpendicular mode at the \bar{M}' point (\square) and of the longitudinal mode at the \bar{M}' point (Δ) and at its local maximum close to the \bar{K} point (∇). (a) Variation of the phonon energies with the Xe distance b_{Xe} by changing the separation between close-packed, $[1\bar{1}0]$ -oriented Xe atomic rows (cf. Fig. 1) but keeping the Xe interatomic distance along the $[1\bar{1}0]$ -oriented rows constant at $a_{\text{Xe}} = 4.4 \text{ \AA}$. (b) Variation of the phonon energies with the Xe distance a_{Xe} along the $[1\bar{1}0]$ -oriented Xe rows, keeping the separation between neighboring rows fixed at the commensurate distance $b_{\text{Cu}} = 3.61 \text{ \AA}$.

stabilized by the substrate corrugation, i.e., the lateral variation of the Cu-Xe binding energy. In particular, the perfect registry along the [001] direction indicates a significant corrugation across the close-packed Cu rows. This corrugation can be easily taken into account in the phonon calculation: It contributes a constant term φ''_{corr} (the second derivative of the corrugation potential) to the dynamical matrix, affecting the phonons polarized within the surface plane. The main effect is the appearance of a phonon gap at the center of the Brillouin zone ($\bar{\Gamma}$).¹⁷ However, the corrugation along the [001] direction will only affect the longitudinal mode along that direction, while the dispersion of the longitudinal mode along the [1 $\bar{1}$ 0] direction studied here is influenced only by the much weaker corrugation along the close-packed [1 $\bar{1}$ 0] direction. A stability analysis of the HOC structures¹⁸ leads to the conclusion that the corrugation along the [1 $\bar{1}$ 0] direction is of the order of 2 meV. Assuming a sinusoidal shape for the corrugation function, a peak-to-peak amplitude of 2 meV would introduce a phonon gap

$\sqrt{\varphi''_{\text{corr}}/M_{\text{Xe}}}$ for the longitudinal mode along this direction of 0.44 meV. Since a constant corrugation term in the dynamical matrix contributes a constant to the *square* of the phonon frequencies, the higher phonon energies away from the center of the Brillouin zone are even less affected,

$$\omega_{\text{corr}} = \sqrt{\omega^2 + \varphi''_{\text{corr}}/M_{\text{Xe}}} . \quad (1)$$

Here ω_{corr} and ω denote the phonon frequencies with and without including the corrugation and M_{Xe} is the mass of a Xe atom. According to (1), the energy shift of the dispersion curve after including a corrugation of 2 meV in the “interesting” region of the longitudinal dispersion curve (where $\hbar\omega \geq 3$ meV) will be ≤ 0.03 meV. This shift is substantially smaller than the experimental accuracy of about 0.2 meV. A substrate corrugation of a few meV along the [1 $\bar{1}$ 0] direction, therefore, does not affect the quantitative results obtained above concerning the role of the lattice distortion on the phonon dispersion.

- ¹K. D. Gibson and S. J. Sibener, *Phys. Rev. Lett.* **55**, 1514 (1985).
²P. Zeppenfeld, K. Kern, U. Becher, R. David, and G. Comsa, *J. Electron Spectrosc.* **54/55**, 265 (1990).
³L. Yang, T. S. Rahman, G. Bracco, and R. Tatarek, *Phys. Rev. B* **40**, 12271 (1989).
⁴S. Lehwald, F. Wolf, H. Ibach, B. M. Hall, and D. L. Mills, *Surf. Sci.* **192**, 131 (1987); P. Zeppenfeld, K. Kern, R. David, K. Kuhnke, and G. Comsa, *Phys. Rev. B* **38**, 12329 (1988).
⁵R. David, K. Kern, P. Zeppenfeld, and G. Comsa, *Rev. Sci. Instrum.* **57**, 2771 (1986).
⁶B. Poelsema and G. Comsa, in *Scattering of Thermal Energy Atoms*, edited by G. Höhler, Springer Tracts in Modern Physics Vol. 115 (Springer, Berlin, 1989).
⁷K. Kern and G. Comsa, in *Kinetics of Ordering and Growth at Surfaces*, edited by M. G. Lagally (Plenum, New York, 1990), p. 53.
⁸B. F. Mason and B. R. Williams, *Surf. Sci.* **130**, 295 (1983).
⁹K. D. Gibson, S. J. Sibener, B. Hall, D. L. Mills, and J. E. Black, *J. Chem. Phys.* **83**, 7893 (1985).
¹⁰B. Hall, D. L. Mills, P. Zeppenfeld, K. Kern, U. Becher, and G. Comsa, *Phys. Rev. B* **40**, 6326 (1989).
¹¹B. Hall, D. L. Mills, P. Zeppenfeld, K. Kern, U. Becher, and

G. Comsa, *Phys. Rev. B* **40**, 6326 (1989).

- ¹²C. Girardet and P. N. M. Hoang, *Surf. Sci.* **282**, 188 (1993).
¹³Phonons polarized in the surface plane of physisorbed monolayers have been measured previously using inelastic neutron scattering; see, e.g., V. L. P. Frank, H. J. Lauter, and P. Leiderer, *Phys. Rev. Lett.* **61**, 436 (1988); and J. M. Layet, M. Bienfait, C. Ramseyer, P. N. M. Hoang, G. Girardet, and G. Coddens, *Phys. Rev. B* **48**, 9045 (1993). However, since microcrystalline substrates have to be used with this technique, the measured phonon density of states are always weighted averages over all possible orientations of the microcrystals and, hence, the fundamental surface phonon-dispersion curves cannot be obtained directly.
¹⁴J. A. Barker, in *Rare Gas Solids*, edited by M. L. Klein and J. A. Venables (Academic, London, 1976), Vol. 1.
¹⁵A. Glachant, M. Jaubert, M. Bienfait, and G. Boato, *Surf. Sci.* **115**, 219 (1981).
¹⁶W. Berndt, *Surf. Sci.* **219**, 161 (1989).
¹⁷J. E. Black, D. L. Mills, W. Daum, C. Stuhlmann, and H. Ibach, *Surf. Sci.* **217**, 529 (1989); J. Black and D. L. Mills, *Phys. Rev. B* **42**, 5610 (1990).
¹⁸C. Ramseyer, C. Girardet, P. Zeppenfeld, J. George, M. Büchel, and G. Comsa, *Surf. Sci.* **313**, 251 (1994).

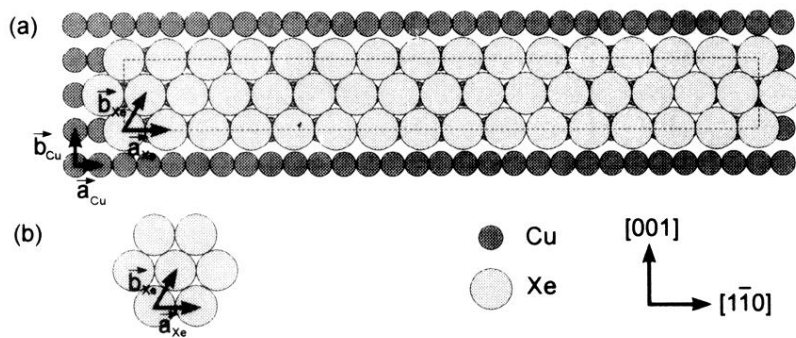


FIG. 1. (a) Model of the (26×2) HOC phase of a Xe monolayer on Cu(110). The xenon atoms are arranged in a quasihexagonal structure; the HOC unit cell is indicated by the dashed lines. In order to fit on the rectangular substrate lattice the Xe layer is compressed along the $[001]$ direction and stretched along the $[1\bar{1}0]$ direction with respect to the floating 2D Xe phase ($a_{Xe} = 4.36 \text{ \AA}$) shown in (b). It is not known whether the Xe atoms on Cu(110) are bound on top of the Cu rows, as shown here, or in the Cu troughs.